Coordination Chemistry Reviews, 123 (1993) 201–228

Luminescent lanthanide complexes as photochemical supramolecular devices

Nanda Sabbatini, Massimo Guardigli
Department of Chemistry "G. Ciamician", University of Bologna, 40126 Bologna (Italy)

Jean-Marie Lehn
Institut Le Bel, Université Louis Pasteur, F-67000 Strasbourg (France)

(Received 19 June 1992)

CONTENTS

A. INTRODUCTION

The design of complexes of lanthanide ions with encapsulating ligands is an important theme in the field of supramolecular chemistry because it offers the possibility to obtain stable luminescent compounds. A relevant aspect of this research consists in the possibility to optimize the luminescence properties of the metal ion by a suitable choice of ligands [1].

This review illustrates the state-of-the-art of the photophysical properties of complexes of lanthanide ions with encapsulating ligands* and their possible use as

---

Correspondence to: Dr. N. Sabbatini, Department of Chemistry "G. Ciamician", University of Bologna, 40126 Bologna, Italy.

* Part of the results have been reviewed in ref. 2.

0010-8545/93/$24.00

luminescent labels in fluoroimmunoassay. For several representative complexes, we will analyze and compare the quantities that determine the metal luminescence, i.e. ligand absorption, ligand-to-metal energy transfer, and decay rate constants of the metal emitting states. In particular, an unified view of the ligand–metal interaction in the excited state will be given via a detailed analysis of the efficiencies of energy conversion from the excited states of the ligands to the emitting states of the metal ions.

B. LUMINESCENCE OF LANTHANIDE IONS

The basic principles related to the excited-state properties of lanthanide ions have been extensively described in many monographs [3–7]. Here we will illustrate only those concepts that are essential to discuss the luminescence properties of the systems dealt with in the following sections.

The importance of the luminescence of lanthanide ions is related to its peculiar characteristics, e.g. long lifetime and line-like emission bands, which make these ions unique among the species that are known to luminesce. Such characteristics are due to the fact that the emitting excited state and the ground state have the same f^n electronic configuration and that the f orbitals are shielded from the environment by the outer s and p electrons.

The $4f^n$ electronic configuration of a lanthanide ion gives rise to several terms whose energies are determined by a combination of interelectronic repulsion, spin-orbit coupling, and, in a coordination environment, ligand field. The electrostatic interaction yields terms with separations of the order of 10^4 cm^{-1}. The spin-orbit interaction then splits these terms into J states, with typical splitting of 10^3 cm^{-1}. Finally, the J degeneracy of the free ion states is partially or fully removed in coordination compounds by the ligand field, the splitting being of the order of 10^2 cm^{-1}.

Transitions between states of f^n configuration are strictly parity forbidden. The probability of such transitions is so low that the molar absorption coefficients are of the order of 1 and the radiative lifetimes are in the millisecond time scale [8]. Actually, the experimental decay times are one or two orders of magnitude lower than the estimated radiative lifetimes. This fact indicates that the decay of the emitting state is mainly governed by non-radiative transitions. According to the theory of non-radiative transitions in lanthanide complexes [4,5,9], the non-radiative relaxation between various J states may occur by interaction of the electronic levels of the lanthanide ion with suitable vibrational modes of the environment. The efficiency of these processes depends on the energy gap between the ground and excited states and the vibrational energy of the oscillators [4,5,10]. When solvents containing O–H groups are coordinated to lanthanide ions, efficient non-radiative deactivations take place via vibronic coupling with the vibrational states of the O–H oscillators [11,12].

If the O—H oscillators are replaced by the low-frequency O—D oscillators, the vibronic deactivation pathway becomes much less efficient.

Horrocks and Sudnick [13,14], by carrying out separate experiments in H_2O and D_2O solutions, have shown that, for the Eu^{3+} and Tb^{3+} complexes, the number of coordinated water molecules, n, is given, with an estimated uncertainty of 0.5, by eqn. (1) where τ_{H_2O} and τ_{D_2O} are the experimental excited-state lifetimes (in ms) in H_2O and D_2O solutions and q is 1.05 and 4.2 for the Eu^{3+} and Tb^{3+} compounds, respectively. The q values show that the vibronic coupling is more effective for the Eu^{3+} than the Tb^{3+} ion, as expected on the basis of the energy gap between the ground and the excited states.

$$n=q\left(\frac{1}{\tau_{H_2O}}-\frac{1}{\tau_{D_2O}}\right) \tag{1}$$

On the assumption that methanol behaves like half a water molecule, Horrocks and co-workers [15] have proposed the use of eqn. (2) to determine the number of coordinated methanol molecules, where τ_{MeOH} and τ_{MeOD} are the excited-state lifetimes (in ms) in MeOH and MeOD solutions and r is 2.1 and 8.4 for the Eu^{3+} and Tb^{3+} compounds, respectively.

$$n=r\left(\frac{1}{\tau_{MeOH}}-\frac{1}{\tau_{MeOD}}\right) \tag{2}$$

The emitting level may also deactivate non-radiatively via thermally activated crossing to short-lived, upper-lying excited states of other configurations (e.g. ligand-to-metal charge-transfer states for the Eu^{3+} complexes [16]). Taking into account the radiative and non-radiative deactivation processes described above, the overall decay rate constant of the luminescent level can be expressed by eqn. (3) where k_r is the radiative rate constant and k_{nr} and $k_{nr}(T)$ are the non-radiative temperature independent and temperature dependent decay rate constants, respectively.

$$k=\frac{1}{\tau}=k_r+k_{nr}+k_{nr}(T) \tag{3}$$

In solvents containing the O—H group, the most important contribution to the k_{nr} term comes from the coupling with the high-energy O—H oscillators. The overall decay constant can thus be rewritten as in eqn. (4)

$$k=\frac{1}{\tau}=k_r+k_{nr}(T)+k_{nr}(OH)+k_{nr}(\text{other vibr.}) \tag{4}$$

where the term k_{nr}(other vibr.) accounts for the radiationless decay via coupling with vibrations different from O—H. The values of the decay rate constants may be obtained from lifetime measurements in hydrogenated (τ_H) and deuterated (τ_D) solvents at different temperatures. On the assumption that (i) the term k_{nr}(other vibr.)

is negligible, (ii) the coupling with the O−D oscillators is completely inefficient, and (iii) at 77 K thermally activated decay processes do not play any role, the radiative rate constant k_r is given by eqn. (5) and the non-radiative rate constants $k_{nr}(T)$ and $k_{nr}(OH)$ at room temperature (hereafter indicated as 300 K) may be evaluated as in eqns. (6) and (7).

$$k_r = \frac{1}{\tau_D^{77K}} \tag{5}$$

$$k_{nr}(T) = \frac{1}{\tau_D^{300K}} - \frac{1}{\tau_D^{77K}} \tag{6}$$

$$k_{nr}(OH) = \frac{1}{\tau_H^{300K}} - \frac{1}{\tau_D^{300K}} \tag{7}$$

When the emitting state is in equilibrium with other excited states, a more complex, non-exponential decay is expected to take place (however, an exponential decay can be generally used in the first approximation). In this case, eqn. (6) does not give $k_{nr}(T)$, but merely a number which reflects the importance of the equilibrium on luminescence.

We can conclude that the coordination environment affects the luminescence intensity and lifetime via the presence of (i) solvent molecules coordinated to the metal ion and (ii) low-lying, short-lived excited states. Non-radiative losses can therefore be controlled by an appropriate choice of the coordination environment of the lanthanide ion.

The luminescence intensity, in addition to depending on the competition between radiative and non-radiative deactivations discussed above, is related, of course, to the efficiency of light absorption. We will see in the following section that supramolecular chemistry offers the opportunity to design stable lanthanide complexes capable of playing the role of molecular devices for efficient light absorption and luminescence emission.

C. ANTENNA EFFECT

As is known [4], lanthanide ions show very small absorption coefficients in the visible and UV spectral region. In coordination chemistry, this drawback may be overcome, in principle, using complexes in which light absorption is performed in ligand-centered or charge-transfer bands. However, lanthanide ions do not exhibit strong coordination ability because of their electronic configuration. For these reasons, conventional ligands are not able to give rise to inert complexes, especially in aqueous solution where solvent molecules efficiently compete to occupy coordination sites. Recent developments in the field of supramolecular chemistry permit rationalization of the synthesis of ligands suitable for lanthanide complexation. A paradigmatic example of complexes of lanthanide ions is the class of cryptates [17–19]. In fact, the cryptand ligands possess spheroidal cavities and binding sites which are "hard" in nature, like oxygens and nitrogens. Potential applications of this type of ligand make use of the high stability of their complexes and their capability of shielding the encapsulated ion from interaction with the surroundings.

In complexes of lanthanide ions with encapsulating ligands, an intense luminescence of the ion may, in principle, be obtained by the "antenna effect" [19–23], which is defined as a light conversion process via an absorption-energy transfer-emission sequence involving distinct absorbing (ligand, light collector) and emitting (metal ion) components (Fig. 1). In such a process, the quantities that contribute to the luminescence intensity are (i) the intensity of the ligand absorption, (ii) the efficiency of the ligand-to-metal energy transfer, and (iii) the efficiency of the metal luminescence.

The efficiency of the energy transfer process between the singlet excited state (obtained by light absorption) of the ligand and the emitting state of the metal, $\eta_{\text{en.tr.}}$, cannot be measured directly. However, it can be obtained, eqn. (8), from the ratio between the quantum yield upon ligand excitation, Φ, and the quantum yield upon metal excitation, Φ_M. When this last quantity cannot be measured, an estimate of its

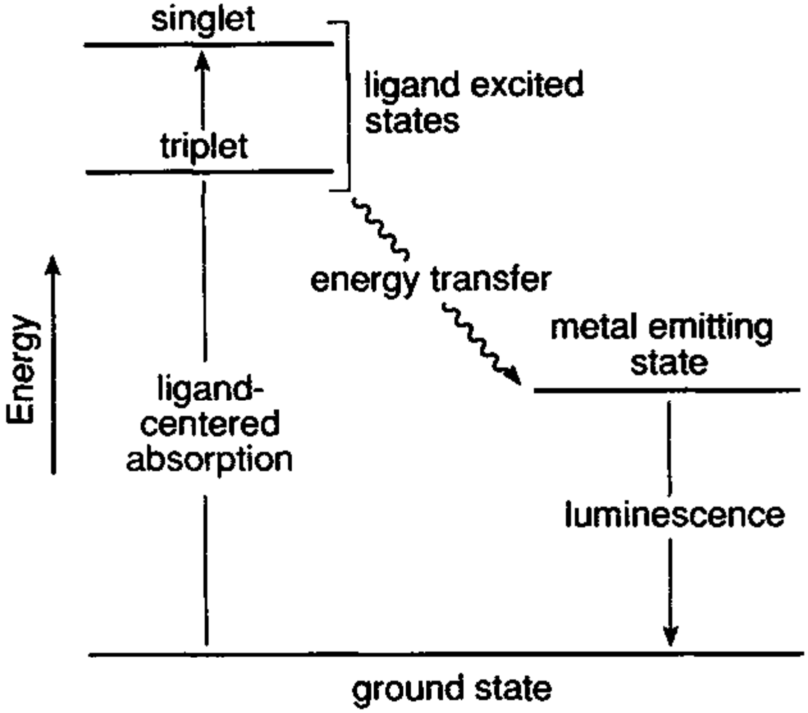

Fig. 1. Schematic representation of the antenna effect involving absorbing ligand and emitting metal subunits.

value can be obtained from eqn. (9) with the assumption that the decay process at 77 K in deuterated solvents is purely radiative.

$$\eta_{\mathrm{en.tr.}} = \frac{\Phi}{\Phi_{\mathrm{M}}} \tag{8}$$

$$\Phi_{\mathrm{M}} = \frac{\tau_{\mathrm{exp.}}}{\tau_{\mathrm{D}}^{77\mathrm{K}}} \tag{9}$$

In the presence of equilibria involving the emitting state and other excited states which decay directly to the ground state, eqn. (9) is not valid and substitution of $\tau_{\mathrm{exp.}}/\tau_{\mathrm{D}}^{77\mathrm{K}}$ for Φ_{M} in eqn. (8) gives a lower limiting value of $\eta_{\mathrm{en.tr.}}$.

D. FLUOROIMMUNOASSAY

Of special interest is the use of lanthanide complexes as luminescent labels in immunology [24–26]. The immunological methods for the determination of biological materials are far superior to almost all other methods as far as sensitivity and specificity are concerned. They are used particularly for the clinical investigation of compounds that are in very low concentrations and for which chemical methods are not sufficiently specific.

The immunological method based on the use of luminescent labels is called fluoroimmunoassay [24]. It consists of the labelling of samples with fluorescent species and the measurement of the luminescence. Fluoroimmunoassay has recently become competitive with radioimmunoassay, which is still the most widely used, even though it presents some drawbacks related to radioactivity. Fluorimetric labelling is relatively inexpensive and is not dangerous, and fluorescence can be measured quickly and simply. However, the use of fluorescent labels to replace radioactive isotopes is hindered by the decreased sensitivity obtained with fluorescence. This is caused, to a great extent, by the sample's (e.g. serum's) own fluorescence. The intensity of this background is affected by the many fluorescent compounds present in the sample, which in addition increase the scattering. Special consideration must be given to the possibility of enhancing sensitivity by using time-resolved fluorimetric immunoassay (TR-FIA).

The principle of this assay takes advantage of sensitized Eu^{3+} or Tb^{3+} luminescence. Since the background luminescence of biological materials is usually short-lived, the Eu^{3+} and Tb^{3+} complexes present the advantage that their emitting states have long luminescence lifetimes. Indeed, a delay is set between the excitation pulse and the measurement of the lanthanide luminescence. In this way, interference from the luminescence of the biological material and from any other material used in the analysis is minimized.

Commercial kits presently available make use of Eu^{3+} chelates. The method involves two steps in which two different europium chelates are used. The first one (e.g. the EDTA chelate) makes sure that the Eu^{3+} ion is strongly bound to the immunoreactive component. The EDTA chelate is then dissociated at low pH and the Eu^{3+} ion is complexed by the second chelating ligand, usually a β-diketone, to give the luminescent complex.

A different, more promising approach to fluoroimmunoassay is based on the use of complexes of lanthanides with encapsulating ligands. The design of complexes which are simultaneously stable and luminescent makes possible, in principle, a one-step procedure. A water-soluble label would avoid problems introduced by the very low solubility of β-diketonates. Finally, higher sensitivity could be achieved by designing strongly luminescent complexes based on the antenna effect (see Sect. B).

E. COMPLEXES OF ENCAPSULATING LIGANDS

This section reviews the photophysical properties of encapsulation complexes of lanthanide ions, i.e. complexes where the ligand presents a three-dimensional conformation and forms a cage around the metal ion.

(i) 2.2.1 Cryptates

The first example of a photophysical study on complexes of lanthanide ions with cage-type ligands deals with the cryptates of the 2.2.1 ligand (Fig. 2) [27–29].

In the case of the $[Eu \subset 2.2.1]^{3+}$ cryptate, the absorption spectrum presents two relatively intense ($\varepsilon \geqslant 100\ M^{-1}\ cm^{-1}$) bands (Fig. 3). These bands have been ascribed to ligand-to-metal charge-transfer (LMCT) transitions. More specifically, the band at higher energy ($\lambda_{max} = 248$ nm) corresponds to a transition involving the amine nitrogens of the ligand, while the other band ($\lambda_{max} = 298$ nm) involves the ether oxygens. The LMCT bands appear also in the excitation spectrum of the Eu^{3+} luminescence, together with the f–f absorption typical of the Eu^{3+} ion.

The increase in luminescence lifetime on passing from H_2O to D_2O solutions (Table 1B) shows that an efficient radiationless decay is due to coupling with the

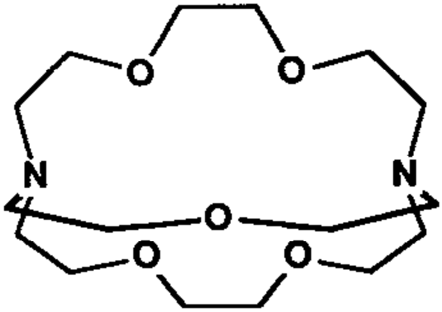

Fig. 2. Schematic representation of the 2.2.1 cryptand.

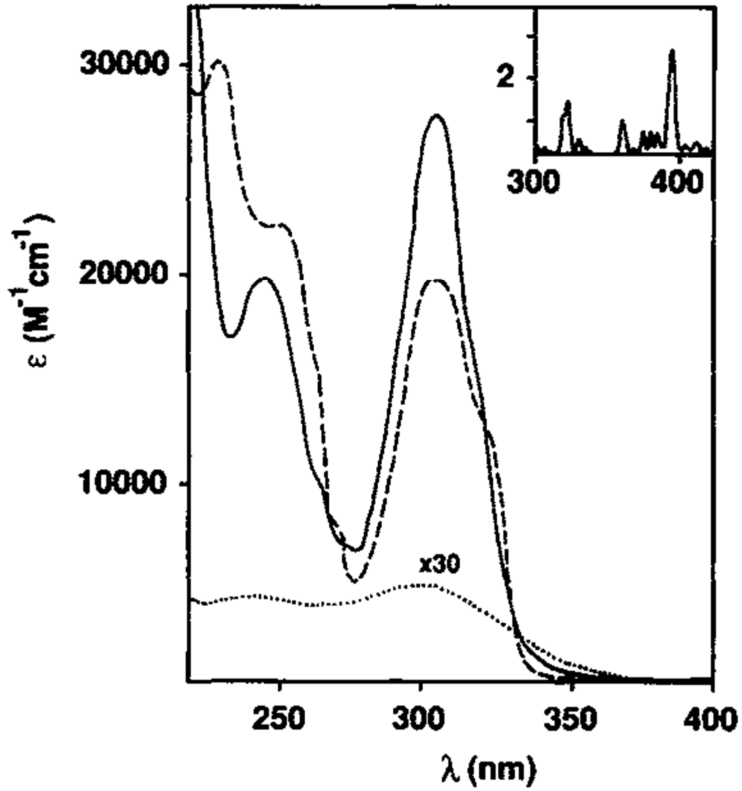

Fig. 3. Absorption spectra of the $[Eu \subset 2.2.1]^{3+}$ (·····), $[Eu \subset \mathbf{2}]^{3+}$ (------), and $[Eu \subset \mathbf{1}]^{3+}$ (——) cryptates in water solutions. Inset: part of the absorption spectrum of the Eu^{3+} aquo ion.

high-energy O—H oscillators. By using Horrocks' equation [13,14], it was estimated that ~3 water molecules coordinate the metal ion in the complex, indicating that the Eu^{3+} ion is markedly shielded from interactions with solvent molecules (the Eu^{3+} aquo ion coordinates 9 to 10 water molecules [30]).

The temperature dependence of the lifetime indicates the presence of a thermally activated decay process. Such a process involves the population of the LMCT excited states from the $^5D_0$ Eu^{3+} emitting state, followed by efficient non-radiative decay to the ground state [28]. As far as the emission quantum yield upon excitation in the $^5L_6$ f–f band is concerned, its low value has been ascribed to deactivation of both the $^5L_6$ and $^5D_0$ Eu^{3+} levels via the low-lying LMCT states [28]. The emission quantum yield upon excitation in the LMCT absorption is even lower, showing that the efficiency of conversion of the charge-transfer excited states into the $^5D_0$ Eu^{3+} emitting state is very low. The role played by the LMCT states in the deactivation of the Eu^{3+} emitting level is clearly pointed out by the photophysical behaviour of the ion pairs between the $[Eu \subset 2.2.1]^{3+}$ cryptate and the fluoride anions [31]. Since the Eu^{3+} ion becomes more difficult to reduce when coordinated to F^- anions, in the ion pairs the LMCT states shift to higher energies (the shift is ~2000 cm^{-1} for $[\mathrm{Eu}\subset 2.2.1]^{3+}-\mathrm{F}^-$ and ~3200 cm^{-1} for $[\mathrm{Eu}\subset 2.2.1]^{3+}-2\mathrm{F}^-$), so that they become less efficient in deactivating the $^5\mathrm{D}_0$ Eu^{3+} emitting level.

TABLE 1

A. Metal luminescence of the Eu^{3+} and Tb^{3+} 2.2.1 cryptates and their ion pairs with fluoride anions

Compound	Lifetime[a]				Quantum yield	Ref.
	$\tau^{300\mathrm{K}}_{\mathrm{H_2O}}$ (ms)	$\tau^{300\mathrm{K}}_{\mathrm{D_2O}}$ (ms)	$\tau^{77\mathrm{K}}_{\mathrm{H_2O}}$ (ms)	$\tau^{77\mathrm{K}}_{\mathrm{D_2O}}$ (ms)	$\Phi^{300\mathrm{K}}$	
$[\mathrm{Eu}\subset 2.2.1]^{3+}$	0.22	0.64	0.34	1.2	0.03[b,c]	27
					0.003[b,d]	27
$[\mathrm{Eu}\subset 2.2.1]^{3+}-\mathrm{F}^-$	0.50	1.5	0.62	1.5		31
$[\mathrm{Eu}\subset 2.2.1]^{3+}-2\mathrm{F}^-$	1.0	1.7	1.2	1.8	1.0[b,c]	31
					0.004[b,d]	31
$[\mathrm{Tb}\subset 2.2.1]^{3+}$	1.3	3.1	1.3	3.1	0.30[e]	29
$[\mathrm{Tb}\subset 2.2.1]^{3+}-\mathrm{F}^-$	1.8	3.4	2.2	3.4		31
$[\mathrm{Tb}\subset 2.2.1]^{3+}-2\mathrm{F}^-$	3.1	3.9	3.7	4.2		31

[a] Measured in correspondence with the most intense metal emission band ($^5\mathrm{D}_0\rightarrow{}^7\mathrm{F}_2$ for Eu^{3+} and $^5\mathrm{D}_4\rightarrow{}^7\mathrm{F}_5$ for Tb^{3+}).

[b] In $\mathrm{D_2O}$ solution.

[c] Excitation in the metal centred $^7\mathrm{F}_0\rightarrow{}^5\mathrm{L}_6$ Eu^{3+} absorption ($\lambda=393$ nm).

[d] Excitation in the low-energy LMCT absorption band ($\lambda_{\max}=298$ nm).

[e] In water solution; excitation in f–f Tb^{3+} absorption ($\lambda=370$ nm).

B. Decay rate constants of the metal emitting state for the Eu^{3+} and Tb^{3+} 2.2.1 cryptates and their ion pairs with fluoride anions[a]

Compound	k_r	$k_{nr}(\mathrm{T})$[b]	$k_{nr}(\mathrm{OH})$	n[c]	Ref.
$[\mathrm{Eu}\subset 2.2.1]^{3+}$	830	730	3000	3.1	28
$[\mathrm{Eu}\subset 2.2.1]^{3+}-\mathrm{F}^-$	670	<50	1330	1.4	20,31
$[\mathrm{Eu}\subset 2.2.1]^{3+}-2\mathrm{F}^-$	560	<50	410	<0.5	31
$[\mathrm{Tb}\subset 2.2.1]^{3+}$	320	<50	450	1.9	20
$[\mathrm{Tb}\subset 2.2.1]^{3+}-\mathrm{F}^-$	290	<50	260	1.1	
$[\mathrm{Tb}\subset 2.2.1]^{3+}-2\mathrm{F}^-$	240	<50	70	<0.5	20

[a] In water solution.

[b] The involvement of the LMCT states in the decay process could imply an equilibrium between these states and the $^5\mathrm{D}_0$ Eu^{3+} emitting state, thus making the use of eqn. (6) inappropriate. However, since the emission quantum yield upon excitation in the LMCT bands is very low, the effect of such an equilibrium, if any, is presumably small.

[c] Number of coordinated $\mathrm{H_2O}$ molecules, estimated using the Horrock's equation [13,14].

The photophysical properties of the $[\mathrm{Eu}\subset 2.2.1]^{3+}$–$\mathrm{F}^-$ and $[\mathrm{Eu}\subset 2.2.1]^{3+}$–$2\mathrm{F}^-$ ion pairs are reported in Table 1A. In the $[\mathrm{Eu}\subset 2.2.1]^{3+}$–$2\mathrm{F}^-$ ion pair, the quantum yield in D_2O solution upon $^5L_6$ f–f excitation is unity and no temperature dependence of the lifetime is observed for both the 1:1 and 1:2 ion pairs (see also the $k_{nr}(T)$ values in Table 1B). This indicates that the energies of the LMCT states become sufficiently high to cancel any contribution of these states to deactivation processes. The shift of the LMCT states can also explain the trend observed in the k_r values (Table 1B). In fact, the mixing of these states with the $^5D_0$ Eu^{3+} emitting state becomes less effective in going from the $[\mathrm{Eu}\subset 2.2.1]^{3+}$ cryptate to the $[\mathrm{Eu}\subset 2.2.1]^{3+}$–$2\mathrm{F}^-$ ion pair because of the increased energy gap. Another interesting effect showed by ion pairing with F^- anions is that the F^- ions effectively replace the water molecules still coordinated to the Eu^{3+} ion in the cryptate (see n values in Table 1B).

Concerning the $[\mathrm{Tb}\subset 2.2.1]^{3+}$ cryptate [29], its absorption spectrum does not differ appreciably from that of the Tb^{3+} aquo ion. As observed for the $[\mathrm{Eu}\subset 2.2.1]^{3+}$ cryptate, the lifetimes in H_2O and D_2O solutions (Table 1A) indicate the presence of a vibronic deactivation mechanism via the O–H groups. In D_2O solutions, the lifetime is temperature-independent (Table 1A), in agreement with the expectation that the Tb^{3+} cryptate does not possess low-lying, excited configuration levels. The absence of low-lying excited states may also explain the much higher quantum yield (Table 1A) found for the $[\mathrm{Tb}\subset 2.2.1]^{3+}$ cryptate compared with the $[\mathrm{Eu}\subset 2.2.1]^{3+}$ cryptate.

Analogously to the $[\mathrm{Eu}\subset 2.2.1]^{3+}$, the $[\mathrm{Tb}\subset 2.2.1]^{3+}$ cryptate gives rise to 1:1 and 1:2 ion pairs with the F^- ions. The effects on the luminescence lifetimes are smaller than in the case of the $[\mathrm{Eu}\subset 2.2.1]^{3+}$ cryptate because they only reflect the replacement of some of the coordinated water molecules. The small decrease in the radiative decay rate constants upon coordination of F^- anions (Table 1B) has been attributed to the blue shift of the f–d Tb^{3+} excited states [31].

In conclusion, the results obtained for the 2.2.1 cryptates have shown that cryptand ligands shield the lanthanide ion from interaction with water molecules, thus improving its emitting properties. In the case of the Eu^{3+} ion, important non-radiative losses are introduced because of the low-energy position of the LMCT states.

(ii) Bpy.bpy.bpy cryptates

In order to increase the intensity of the lanthanide luminescence exploiting the antenna effect, complexes with strongly absorbing cryptands have been designed. The prototype of this class of ligands is the bpy.bpy.bpy macrobicyclic cryptand (ligand **1**) containing three 2,2′-bipyridine (bpy) units [32]. It shows intense absorption bands in the UV region due to $\pi\rightarrow\pi^*$ transitions in the bpy units [22]. Some lanthanide bpy.bpy.bpy cryptates were obtained [19,33] from the

$[\mathrm{Na} \subset \mathrm{bpy.bpy.bpy}]^{+}$ cryptate and the crystal structures have been determined [34]. Their absorption spectra (Fig. 3) show bands due to the same transitions present in the free bpy, but some red shift and decrease in absorption intensity are observed.

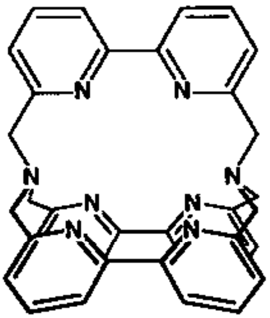

1

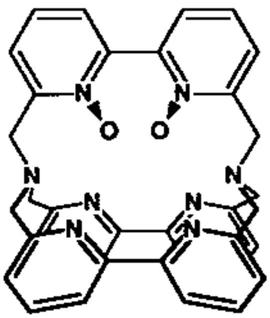

2

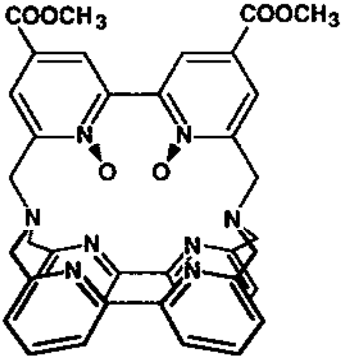

3

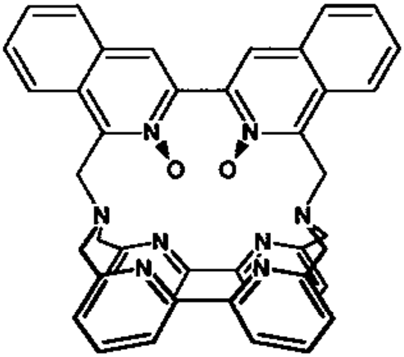

4

The photophysical behaviour of the Eu^{3+} and Tb^{3+} complexes with this ligand has been investigated in solution [19–22,35] and in the solid state [36,37]. The conclusions of such a study are summarized in the following.

In the $[\mathrm{Eu} \subset \mathbf{1}]^{3+}$ and $[\mathrm{Tb} \subset \mathbf{1}]^{3+}$ cryptates, an energy transfer process from the ligand to the metal ion takes place. However, the rather low values of the emission quantum yields (Table 2) indicate that the light absorbed in the ligand is not converted efficiently into light emitted by the metal ion. In order to understand the factors that determine the non-radiative losses, the temperature and solvent dependence of the lifetimes of the metal luminescence (Table 2) as well as the photophysical properties of the ligand were investigated [22].

For both the $[\mathrm{Eu} \subset \mathbf{1}]^{3+}$ and $[\mathrm{Tb} \subset \mathbf{1}]^{3+}$ cryptates, comparison of the lifetimes

TABLE 2

Luminescence lifetimes and quantum yields[a]

Compound	Lifetime[b]				Quantum yield[c]		Ref.
	τ_H^{300K} (ms)	τ_D^{300K} (ms)	τ_H^{77K} (ms)	τ_D^{77K} (ms)	Φ_H^{300K}	Φ_D^{300K}	
$[\mathrm{Eu}\subset\mathbf{1}]^{3+}$	0.34	1.7	0.81	1.7	0.02	0.10	22
$[\mathrm{Eu}\subset\mathbf{2}]^{3+}$	0.46	1.15	1.2	1.3	0.15	0.30	39
$[\mathrm{Eu}\subset\mathbf{3}]^{3+}$	0.40	0.70	0.80	1.1	0.09	0.17	40
$[\mathrm{Eu}\subset\mathbf{4}]^{3+}$	0.39	0.66	1.0	1.1	0.20	0.30	39
$[\mathrm{Eu}\subset\mathbf{5a}]^{3+}$	1.5	1.9	1.8	1.9	0.10	0.20	44
$[\mathrm{Eu}\subset\mathbf{5b}]^{3+}$ [d]	1.0	1.8	1.3	2.0	0.01	0.01	44
$[\mathrm{Eu}\subset\mathbf{6}]^{3+}$	0.50	1.2	1.2	1.45	0.015	0.035	40
$[\mathrm{Eu}\subset\mathbf{7}]^{3+}$	0.50	0.57	0.87	1.1	0.05	0.07	45
$[\mathrm{Eu}\subset\mathbf{8}]^{3+}$ [d]	0.95	1.8	0.94	2.0	0.06	0.10	47
$[\mathrm{Eu}\subset\mathbf{9}]^{3+}$	0.34	1.8	[e]	[e]	0.003	0.014	47
	0.81[d]	1.7[d]	1.1[d]	1.8[d]	0.07[d]	0.20[d]	47
$[\mathrm{Eu}\subset\mathbf{10}]^{3+}$	0.65	1.9	1.8	2.0	0.0002		49
$[\mathrm{Tb}\subset\mathbf{1}]^{3+}$	0.45[f]	0.63[f]	1.7	3.8	0.03	0.03	22
	0.33	0.43					20
$[\mathrm{Tb}\subset\mathbf{5a}]^{3+}$ [d]	1.1	1.2	2.0	2.9	0.14	0.35	44
$[\mathrm{Tb}\subset\mathbf{7}]^{3+}$	1.5	1.5	1.4	1.5	0.37	0.38	45
$[\mathrm{Tb}\subset\mathbf{10}]^{3+}$	1.5	2.6	1.6	2.8	0.20	0.30	49

[a] In aerated water solution unless otherwise noted.

[b] Measured in correspondence with the emission bands $^5D_0 \rightarrow {}^7F_2$ and $^5D_4 \rightarrow {}^7F_5$ for Eu^{3+} and Tb^{3+}, respectively.

[c] Excitation in ligand-centred bands.

[d] In methanol solution.

[e] The measurement was prevented by the weakness of the luminescence signal.

[f] In deaerated solution.

and quantum yields in H_2O and D_2O solutions indicates that non-radiative deactivations via the O—H vibrations take place. It has been estimated that ~2.5 water molecules are coordinated to the metal ions.

In the $[\mathrm{Tb}\subset\mathbf{1}]^{3+}$ cryptate, the strong temperature dependence of the lifetime indicates that an important role in the decay of the $^5D_4$ Tb^{3+} emitting state is played by a thermally activated process. Since no CT or f–d states are expected to lie at accessible energies in the complex, it was proposed that the decay involves the triplet excited state of the ligand. In fact, this level lies at 21 600 cm^{-1}, i.e. 1200 cm^{-1} above the Tb^{3+} emitting level, and therefore it may be thermally populated at room temperature. A proof that the $^5D_4$ Tb^{3+} level is in equilibrium with the triplet ligand level is given by the quenching of the Tb^{3+} luminescence by O_2 ($k_q = 3.9 \times 10^6$ M^{-1} s^{-1}). Such a quenching, in fact, does not take place by interaction of O_2 with the excited central metal ion, as indicated by the lack of any O_2 effect on the luminescence of the $[Tb \subset 2.2.1]^{3+}$, $[Eu \subset 2.2.1]^{3+}$ and $[Eu \subset \mathbf{1}]^{3+}$ cryptates, but it reflects the quenching effect of O_2 on the excited bpy moiety. The rate constants obtained for the quenching by O_2 of Tb^{3+} luminescence and triplet bpy absorption ($k_q = 5 \times 10^8$ M^{-1} s^{-1} for $[Gd \subset \mathbf{1}]^{3+}$) are in the ratio expected from the Boltzmann distribution caused by the energy gap of 1200 cm^{-1} between these two levels [22].

A detailed analysis of the decay kinetics has led to the evaluation of the rate constants of processes involved in the equilibrium (Fig. 4). It has been shown that the energy transfer from the triplet level of the ligand to the $^5D_4$ Tb^{3+} excited state is very efficient (in fact $k_2^f/(k_2^f + k_1) \sim 1$) and therefore it is able to compete with the other processes which deactivate the triplet level. The weakness of the observed Tb^{3+} luminescence ($\Phi = 0.03$, Table 2) has been explained as due to the fact that ~100% of the Tb^{3+} excited states undergo back energy transfer to the triplet ligand level, which, even if with low efficiency (~0.01), deactivates to the ground state.

As far as the $[Eu \subset \mathbf{1}]^{3+}$ cryptate is concerned, the situation is quite different. The lifetime depends only slightly on temperature, so that no thermally activated

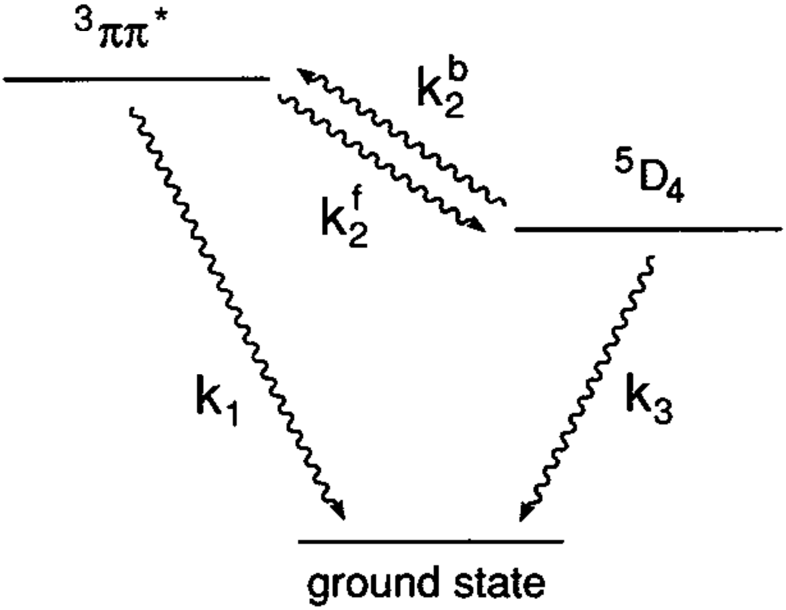

Fig. 4. Kinetic scheme of the equilibrium involved in the decay of the Tb^{3+} luminescent state in the $[Tb \subset \mathbf{1}]^{3+}$ cryptate. k_1 and k_3 represent the sum of the radiative and non-radiative decay rate constants for the ligand triplet and Tb^{3+} $^5D_4$ excited states, respectively. k_2^f is the rate constant for the triplet-to-metal energy transfer and k_2^b is the rate constant for the back energy transfer. The values obtained for these rate constants are $k_1 = 4.3 \times 10^5$ s^{-1}, $k_2^f = 5.0 \times 10^7$ s^{-1}, $k_2^b = 1.6 \times 10^5$ s^{-1}, and $k_3 = 8.9 \times 10^2$ s^{-1} [22].

process may play a substantial role in the decay of the $^5D_0$ Eu^{3+} luminescent level. This is particularly true as far as activation to the triplet ligand excited state is concerned, since such a state lies at about 4000 cm^{-1} above the Eu^{3+} luminescent level.

In spite of the absence of thermally activated decays, the emission quantum yield is rather low for this complex also ($\Phi = 0.1$ in D_2O solution). Assuming that the energy transfer from the triplet ligand excited state to the emitting metal state is as fast as in the $[Tb \subset \mathbf{1}]^{3+}$ cryptate, the non-radiative losses have been ascribed to the population of LMCT states from the singlet ligand excited state [22]. However, the LMCT states could also deactivate the ligand triplet excited state, so that the triplet→metal energy transfer in this complex may be less efficient than in the corresponding Tb^{3+} cryptate.

In the solid state, a considerably higher value of the emission quantum yield (0.5 at room temperature) was obtained for $[Eu \subset \mathbf{1}]^{3+}$ [37]. This is also the case for the $[Tb \subset \mathbf{1}]^{3+}$ cryptate up to about 100 K; at higher temperatures, energy migration and back energy transfer from the metal ion to the cryptand ligand decrease the emission intensity [36].

(iii) N-oxide cryptates

In an attempt to improve the luminescence of the lanthanide bpy.bpy.bpy cryptates, one of the bpy units of the bpy.bpy.bpy cryptand was replaced with the $bpyO_2$ or $biqO_2$ unit [38]. Preliminary results on the luminescence of the $[Eu \subset \mathbf{2}]^{3+}$ and $[Eu \subset \mathbf{4}]^{3+}$ complexes [38] have shown that the included cation is better protected from interaction with water than in the case of the $[Eu \subset \mathbf{1}]^{3+}$ cryptate and that these complexes present a significant gain in light-conversion efficiency over earlier europium cryptates. A detailed photophysical study of the $[Eu \subset \mathbf{2}]^{3+}$ and $[Eu \subset \mathbf{4}]^{3+}$ [39] and $[Eu \subset \mathbf{3}]^{3+}$ [40] complexes was performed in order to characterize quantitatively their luminescence properties.

The absorption spectra of the $[Eu \subset \mathbf{2}]^{3+}$, $[Eu \subset \mathbf{3}]^{3+}$, and $[Eu \subset \mathbf{4}]^{3+}$ complexes show the same bands of the parent cryptates containing only bpy and biq units and shoulders on the red side of the lowest energy bands due, most likely, to $bpyO_2$- and $biqO_2$-localized ligand excited states. In all cases, the molar absorption coefficient at the maximum is lower than in the corresponding cryptates without *N*-oxide groups (Fig. 3).

The observation that the shielding ability of these ligands is superior to that of the bpy.bpy.bpy cryptand is confirmed by the lifetime values in H_2O and D_2O solutions (Table 2). As found in the crystal structure of the $[Eu \subset \mathbf{4}]^{3+}$ cryptate [41], the O sites block the faces of the macrobicyclic structure, thereby preventing the approach of H_2O molecules to the metal ion.

Comparison between the lifetimes at 300 K and 77 K in D_2O solution (Table 2) indicates the presence of a thermally activated decay pathway of the $^5D_0$ Eu^{3+} luminescent level, differently from that observed for the $[Eu \subset \mathbf{1}]^{3+}$ complex. Such a process is rather important for $[Eu \subset \mathbf{3}]^{3+}$ and $[Eu \subset \mathbf{4}]^{3+}$, while it plays a minor role in $[Eu \subset \mathbf{2}]^{3+}$. This decay pathway could involve the population of LMCT excited states (as observed for the $[Eu \subset 2.2.1]^{3+}$ cryptate [28]), which are expected to lie at lower energies than in the parent $[Eu \subset \mathbf{1}]^{3+}$ cryptate (see Discussion). However, in contrast to the $[Eu \subset 2.2.1]^{3+}$ cryptate, the LMCT states cannot be observed in the absorption spectrum because of the overlap with the much more intense ligand-centred bands. This also prevents the possibility of investigating the involvement of an equilibrium between the $^5D_0$ Eu^{3+} luminescent level and the LMCT states in the decay process. In the case of the $[Eu \subset \mathbf{4}]^{3+}$ cryptate, the temperature dependence was explained by taking into account the presence of an equilibrium between the triplet of the 3,3′-biisoquinoline unit and the $^5D_0$ Eu^{3+} level [39]. Such an explanation, however, cannot be valid for the $[Eu \subset \mathbf{2}]^{3+}$ and $[Eu \subset \mathbf{3}]^{3+}$ cryptates because the energy gap between the triplet ligand excited state and the metal emitting state is high and the equilibrium is not possible.

The luminescence quantum yields of these cryptates are considerably higher than for the $[Eu \subset \mathbf{1}]^{3+}$ cryptate, in spite of the presence of an additional decay process. The effect of such a process on the quantum yield is presumably overcome by a more efficient ligand-to-metal energy transfer, due to $bpyO_2$- and $biqO_2$-localized levels (which may give rise to a more efficient population of the lowest triplet level of the ligand) or to a closer approach between the ligand and the metal ion (see Discussion).

(iv) Complexes of branched-macrocyclic ligands

The 2,2′-bipyridine chromophoric group has been used as a building block to synthesize the branched macrocyclic ligands **5a** and **5b** [42], **6** [43], and **7** [42]; some lanthanide complexes of these ligands have been prepared [43–45]. Interestingly, in most cases these ligands shield the metal ion towards interaction with solvent molecules more efficiently than the cryptands.

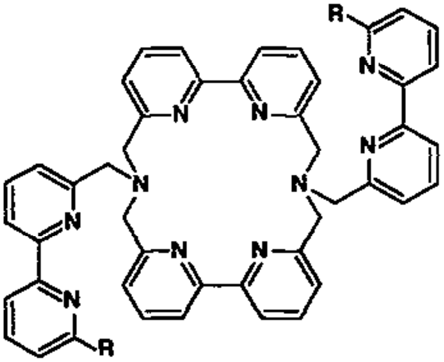

5a : R = H
5b : R = CH_3

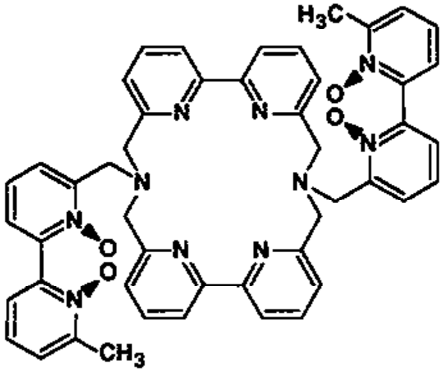

6

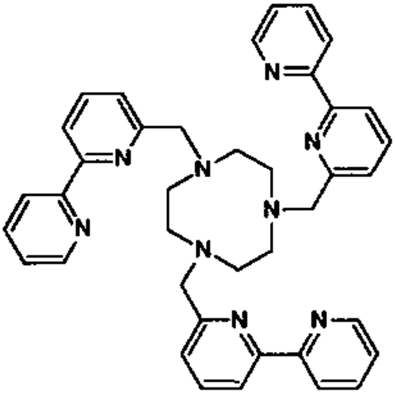

7

For the $[Eu \subset \mathbf{5a}]^{3+}$ complex [44], comparison of the lifetime and quantum yield values in H_2O and D_2O (Table 2) shows that some deactivation via coupling with the O–H vibrations takes place, while no temperature effect is present, analogously to that observed for the $[Eu \subset \mathbf{1}]^{3+}$ cryptate. In contrast to $[Eu \subset \mathbf{5a}]^{3+}$, the corresponding Tb^{3+} complex is unstable in water. The reason for such behaviour was not investigated and the complex was therefore studied in methanol [44]. The lifetime values (Table 2) are almost the same in MeOH and MeOD, while a considerable temperature dependence is observed. A fast metal-to-ligand back energy transfer seems to be an important decay pathway of the $^5D_4$ Tb^{3+} emitting state, as is also the case for the $[Tb \subset \mathbf{1}]^{3+}$ cryptate. However, the high value of the quantum yield ($\Phi = 0.35$ in D_2O) suggests that this process plays a less important role than in the corresponding bpy.bpy.bpy cryptate. The $[Eu \subset \mathbf{5b}]^{3+}$ complex [44] is unstable in water, presumably because the methyl groups prevent a close approach of the branched bpy units to the metal ion, thus allowing the water molecules to compete for ion complexation. In methanol, which is known to be a complexing solvent weaker than water for lanthanide ions, this complex is stable. We can notice that, while the solvent and temperature dependence of the lifetime is analogous to that shown by $[Eu \subset \mathbf{5a}]^{3+}$, the luminescence quantum yield is much smaller, probably because of a reduced efficiency of ligand-to-metal energy transfer due to the presence of the methyl groups [44]. This interpretation is supported by the presence of a residual ligand-centred phosphorescence, which may also be due to an incomplete ligand-to-metal energy transfer involving the branched units. The efficient shielding offered by both the **5a** and **5b** ligands towards solvent interaction indicates that, as expected by examination of space-filling models, the metal ion can be enclosed in the macrocyclic ring and then encapsulated by the two branches of the ligand.

Following the approach described for cryptand ligands, *N*-oxide groups have also been introduced in the ligand **5b**, thus obtaining the ligand **6** [43]. The $[\mathrm{Eu}\subset\mathbf{6}]^{3+}$ and $[\mathrm{Tb}\subset\mathbf{6}]^{3+}$ complexes show remarkable stability in water [40], in contrast to the $[\mathrm{Eu}\subset\mathbf{5b}]^{3+}$ complex. The effect introduced by the *N*-oxide groups is most likely due to their ability to overcome the steric hindrance of the methyl groups. In fact, the O sites of the *N*-oxide groups can approach the Eu^{3+} ion better than the bpy nitrogen of the ligand **5b**, giving rise to a more stable complex in spite of their weaker basicity. As far as the absorption and emission properties of the $[\mathrm{Eu}\subset\mathbf{6}]^{3+}$ complex are concerned [40], the presence of the *N*-oxide group introduces effects analogous to those observed in going from the $[\mathrm{Eu}\subset\mathbf{1}]^{3+}$ cryptate to its *N*-oxide derivatives (Table 2). The corresponding $[\mathrm{Tb}\subset\mathbf{6}]^{3+}$ complex does not show any emission at room temperature, while some emission has been observed at 77 K [40]. The lack of metal luminescence at room temperature is reasonably ascribed to non-radiative deactivation via the triplet state of the ligand, which lies at almost the same energy as the emitting state (for the phosphorescence of the $[\mathrm{Gd}\subset\mathbf{6}]^{3+}$ complex, $\lambda_{\max} \sim 500$ nm [40]).

The Eu^{3+} and Tb^{3+} ions have also been encapsulated in the bpy-branched triazacyclononane ligand 7 and the photophysical properties of the complexes so obtained have been investigated [45]. For both the Eu^{3+} and Tb^{3+} complexes, the lifetimes in H_2O and D_2O solutions are almost the same, showing that no water molecules are coordinated to the metal ions. For the Eu^{3+} complex, the temperature dependence of the lifetime, the short lifetimes and the low quantum yields (Table 2) have been associated with the presence of low-lying LMCT levels involving the aliphatic nitrogens. For the Tb^{3+} complex, the lack of any thermally activated decay process and of coordinated water molecules (see lifetime values in Table 2) leads to a high quantum yield ($\Phi = 0.37$ in H_2O solution). It is interesting to notice that, for this complex, the lifetime at 77 K in D_2O solution is considerably shorter than those usually shown by other Tb^{3+} complexes. This fact has been explained as due to the approximation introduced when k_{nr}(other vibr.) is neglected in eqn. (6). In fact, such a term could be not negligible because of the presence of CH_2 groups which are very close to the metal, so that some coupling with C—H vibrations may be effective. The same considerations should also be valid for the Eu^{3+} complex. However, in this case the presence of effects related to LMCT states makes the comparison with other Eu^{3+} complexes less informative.

Results reported for the Eu^{3+} complex of a macrocycle containing two bpyO_2 units appear to be interesting [46].

(v) Podates

The 2,2′-bipyridine chromophoric unit has also been used to synthesize the tripode and tetrapode ligands **8** and **9** [42].

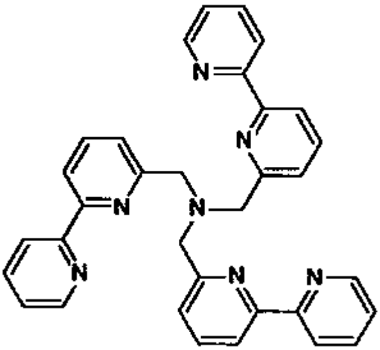

8

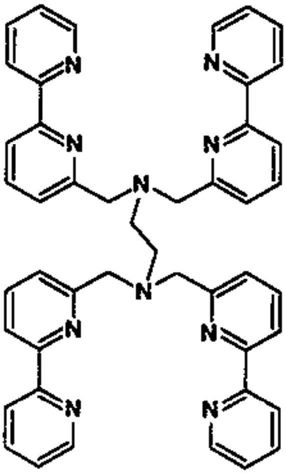

9

The Eu^{3+} complexes of these ligands have also been prepared and their absorption and luminescence properties have been studied [47]. $[Eu \subset \mathbf{8}]^{3+}$ and $[Eu \subset \mathbf{9}]^{3+}$ are quite stable in MeOH solution. In water solution, these compounds undergo decomposition, which, however, is very slow for $[Eu \subset \mathbf{9}]^{3+}$. The absorption spectra of these complexes are identical, except, of course, for a difference in intensity which reflects the different number of bpy units. Some absorption and luminescence data in MeOH and, for $[Eu \subset \mathbf{9}]^{3+}$, in H_2O are gathered in Table 2. Such data show that the temperature-dependent path for deactivation of the luminescent $^5D_0$ level is negligible for both $[Eu \subset \mathbf{8}]^{3+}$ and $[Eu \subset \mathbf{9}]^{3+}$, while deactivation by coupling with the high-energy O–H vibrations is very efficient. The latter deactivation pathway plays a more important role for $[Eu \subset \mathbf{9}]^{3+}$ than for $[Eu \subset \mathbf{8}]^{3+}$, suggesting that the smaller ligand **8** leaves less room for solvent accessibility in the first coordination sphere. It is interesting to notice that, for $[Eu \subset \mathbf{9}]^{3+}$ in D_2O, the lifetime is nearly the same as in MeOD, while the quantum yield is one order of magnitude lower. This behaviour has been attributed to a smaller ligand-to-metal energy-transfer efficiency in water than in methanol due, most likely, to a higher bpy–Eu^{3+} distance in water solution.

(vi) Complexes of functionalized calixarenes

Encapsulation of the Eu^{3+} and Tb^{3+} ions in the *p*-*t*-butylcalix[4]arene tetraacetamide ligand **10** [48] has led to relatively stable, water-soluble complexes, which show interesting luminescence properties [49]. It has been shown that, in these complexes, only one water molecule is coordinated to the metal ion. The absorption spectrum shows two bands at 273 and 282 nm, which correspond to transitions in the aromatic groups of the ligand. The Tb^{3+} complex shows a high luminescence quantum yield upon ligand excitation and a long luminescence lifetime which is temperature-independent. The last observation indicates that no thermally activated process may play a substantial role in the decay of the $^5D_4$ luminescent level. In fact, the triplet excited state of the ligand lies at about 4000 cm^{-1} above the $^5D_4$ Tb^{3+} emitting state.

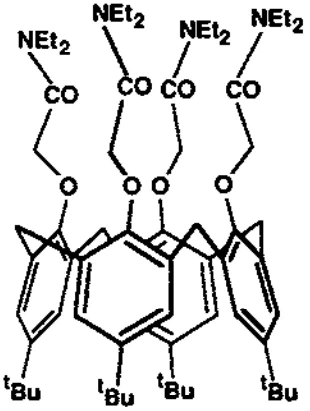

10

For the Eu^{3+} complex, the relatively short lifetime and the very low luminescence quantum yield are ascribed to the presence of ligand-to-metal charge-transfer states (observed as a shoulder around 300 nm in the absorption and excitation spectra) which may efficiently deactivate both the excited states of the ligand and the $^5D_0$ emitting level of the metal to the ground state.

F. DISCUSSION

We would first like to stress the unique features of the complexes examined, especially the cryptates, which combine lanthanide luminescence with the thermodynamic and kinetic stability, the shielding of the included cation and the high absorption coefficient of the encapsulating structures. In this section, the antenna effect shown by these supramolecular photochemical devices will be analyzed in some detail. Ligand absorption, ligand-to-metal energy transfer, and metal luminescence will be discussed on the basis of the data collected in Table 3. In this table, the energy transfer efficiencies and the decay rate constants have been obtained using the experimental data reported in Sect. E.

As far as the absorption properties are concerned, first of all we can notice

TABLE 3

Absorption, energy transfer, and decay characteristics[a]

Compound	λ_{max} (nm)	ε_{max} ($M^{-1}\,cm^{-1}$)	$\eta_{en.tr.}$[b]	k_r (s^{-1})	$k^*_{nr}(T)$[c] (s^{-1})	$k_{nr}(OH)$ (s^{-1})	n[d]
$[\mathrm{Eu}\subset\mathbf{1}]^{3+}$	303	28000	0.10	590	<50	2400	2.5
$[\mathrm{Eu}\subset\mathbf{2}]^{3+}$	304	20000	0.40[e]	770	100[f]	1300	1.4
$[\mathrm{Eu}\subset\mathbf{3}]^{3+}$	306	17000	0.25[e]	900	500[f]	1100	1.1
$[\mathrm{Eu}\subset\mathbf{4}]^{3+}$	304	20000	0.55[e]	900	600[f]	1000	1.1
$[\mathrm{Eu}\subset\mathbf{5a}]^{3+}$	312	36000	0.20	530	<50	140	<0.5[h]
$[\mathrm{Eu}\subset\mathbf{5b}]^{3+}$ [g]	299	39000	0.02	500	50	450	0.9
$[\mathrm{Eu}\subset\mathbf{6}]^{3+}$	310	15500	0.05[e]	700	150[f]	1200	1.2
$[\mathrm{Eu}\subset\mathbf{7}]^{3+}$	311	24500	0.14[e,i]	900[j]	850[f]	250	<0.5
$[\mathrm{Eu}\subset\mathbf{8}]^{3+}$ [g]	301	32000	0.12	500	50	500	1.0
$[\mathrm{Eu}\subset\mathbf{9}]^{3+}$ [g]	301	42000	0.20	550	<50	650	1.4[k]
$[\mathrm{Eu}\subset\mathbf{10}]^{3+}$	273	1100	0.0006	500	<50	1000	1.1
$[\mathrm{Tb}\subset\mathbf{1}]^{3+}$	304	29000	~1[l]	260	1300[f,m]	630	2.7
$[\mathrm{Tb}\subset\mathbf{5a}]^{3+}$ [g]	312	44000	0.80[n]	350	500[f]	80	0.6
$[\mathrm{Tb}\subset\mathbf{7}]^{3+}$	311	20400	0.40[i]	670[j]	<50	<50	<0.5
$[\mathrm{Tb}\subset\mathbf{10}]^{3+}$	273	1100	0.35	360	<50	280	1.2

[a] In water solution unless otherwise noted.

[b] Obtained using eqns. (8) and (9) unless otherwise noted.

[c] This column presents the values obtained using eqn. (6), regardless of the presence of equilibria (see text).

[d] Number of coordinated solvent (water or methanol) molecules, as obtained from the empirical Horrocks' equation in water [13,14] and its modified form for methanol solutions [15].

[e] Calculated on the assumption that the thermally activated decay process does not involve any equilibrium between the metal emitting state and other excited states (see text).

[f] It cannot be excluded that the excited state involved in the thermally activated decay is in equilibrium with the metal emitting state.

[g] In methanol solution. The use of water was prevented by the lability of the complex in this solvent.

[h] In methanol solution, $n=0.5$ is obtained using the lifetime values reported in ref. 44.

[i] A higher value is expected considering that the radiative lifetime may be longer than $\tau^{77K}_{D_2O}$ if vibronic contributions involving C—H bonds are present (see text).

[j] A lower value is expected considering that vibronic contributions involving C—H bonds may be present (see text).

[k] In water solution, $n=2.5$ has been obtained [47].

[l] Obtained from the experimental $\eta_{triplet\rightarrow metal}$ value because the presence of an equilibrium involving the $^5D_4$ Tb^{3+} emitting state prevents the use of eqns. (8) and (9) (see text).

[m] From kinetic data in deaerated solution, a value of $1.6\times10^5\ s^{-1}$ was obtained for the rate constant of the thermally activated back energy transfer from the $^5D_4$ Tb^{3+} emitting state to the lowest triplet state of the ligand [22].

[n] Calculated considering that the equilibrium between the emitting state of the Tb^{3+} ion and the triplet excited state of the ligand, if any, does not play an important role (see text).

that, for complexes of ligands containing only bpy units, appreciable differences in λ_{max} (corresponding to $\pi \rightarrow \pi^*$ absorption bands in 2,2′-bipyridine) are observed. Since complexation gives rise to a red shift of the bpy absorption (for free 2,2′-bipyridine, $\lambda_{max} = 281$ nm [22]), the observed differences may be related to the amount of ligand–metal interaction in the complex. The effect is more pronounced for complexes of branched-macrocyclic ligands (except $[\mathrm{Eu} \subset \mathbf{5b}]^{3+}$, see below), while a smaller red shift is observed in complexes of cryptand or podand ligands. This behaviour may be accounted for by considering that, in complexes of branched-macrocyclic ligands, the approach between the chromophore and the metal ion may be closer than in cryptates and podates. In this connection, the much lower red shift shown by $[\mathrm{Eu} \subset \mathbf{5b}]^{3+}$ compared with $[\mathrm{Eu} \subset \mathbf{5a}]^{3+}$ may be due to the presence of the methyl groups, which prevents a closer ligand–metal approach. Another factor to consider is that angles between the bipyridine groups of the bpy units may be different in the different complexes. Note that the λ_{max} values have been compared regardless of the solvent (water or methanol) used because no spectral shift was observed in these solvents for free 2,2′-bipyridine. The interpretation of the different values obtained for λ_{max} is supported by the parallel trend shown by the number of coordinated solvent molecules (Table 3) which, of course, is related to the complexation properties of the ligand (see below). The introduction of heterocyclic *N*-oxide groups in ligands containing bpy units gives rise to substantial changes in the absorption spectra of their complexes due to the presence of new, low-energy excited states. In particular, the intensity of the absorption maximum decreases, making the ligand a less efficient antenna. The absorption spectra of complexes of the functionalized calixarene **10** are much weaker compared with those of complexes containing bpy units because of the intrinsically different nature of the chromophore.

As far as the ligand-to-metal energy transfer process is concerned, Table 3 presents the energy conversion efficiencies from the absorbing singlet state of the ligand to the emitting state of the metal ion, $\eta_{en.tr.}$, obtained as described in Sect. C (eqns. (8) and (9)). This is the quantity to consider from a practical point of view. The triplet excited state, better than the singlet, is expected to be directly involved in the ligand-to-metal energy transfer because of its much longer lifetime. Therefore, in principle, it is also interesting to know the efficiency of the triplet→metal energy transfer step, $\eta_{triplet \rightarrow metal}$ because it is directly related to the ligand–metal interaction. Among the complexes investigated, this quantity has been measured directly only for the $[\mathrm{Tb} \subset \mathbf{1}]^{3+}$ complex [22]. In the other cases, an estimate may be obtained considering that $\eta_{triplet \rightarrow metal}$ is related to the experimental $\eta_{en.tr.}$ by the equation

$$\eta_{en.tr.} = \eta_{singlet \rightarrow triplet} \eta_{triplet \rightarrow metal} \tag{10}$$

where $\eta_{singlet \rightarrow triplet}$ is the efficiency of singlet→triplet conversion in the complex.

In the absence of decay processes of the singlet excited state to excited states different from the triplet, $\eta_{singlet \rightarrow triplet}$ is at least equal to the intersystem crossing efficiency of the free ligand, η_{isc}, because of the heavy metal effect. In contrast, when in the complex the singlet excited state undergoes deactivation processes related to the presence of the metal, $\eta_{\text{singlet}\rightarrow\text{triplet}}$ may be lower than η_{isc} of the ligand, thus giving a lower limiting value of $\eta_{\text{triplet}\rightarrow\text{metal}}$ if η_{isc} is substituted for $\eta_{\text{singlet}\rightarrow\text{triplet}}$ in eqn. (10).

As mentioned above, for the $[\text{Tb}\subset\mathbf{1}]^{3+}$ complex, the value of $\eta_{\text{triplet}\rightarrow\text{metal}}$ has been obtained experimentally [22]. Interestingly, its value is about 1, showing that, in this complex, the triplet-to-metal energy transfer overcomes the other processes that deactivate the ligand triplet state. A value close to unity is also obtained for $\eta_{\text{en.tr.}}$ if the η_{isc} value for free 2,2′-bipyridine (~1) is substituted for $\eta_{\text{singlet}\rightarrow\text{triplet}}$ in eqn. (10). This substitution appears to be justified if one considers that the Tb^{3+} ion should not introduce low-lying excited states [7], which deactivate the bpy singlet excited state, and the heavy metal ion could only increase the intersystem crossing efficiency. It is interesting to point out the remarkable difference between the $\eta_{\text{en.tr.}}$ value and the emission quantum yield ($\Phi = 0.03$ in D_2O solution at 300 K). Such a difference, due to the equilibrium between the $^5D_4$ Tb^{3+} emitting state and the ligand triplet excited state (see Sect. E), highlights the importance of the metal-to-ligand back energy transfer in determining non-radiative losses. For the $[\text{Tb}\subset\mathbf{5a}]^{3+}$ complex, behaviour analogous to that observed for $[\text{Tb}\subset\mathbf{1}]^{3+}$ is expected, because the energetics of the two systems (whose ligands contain only bpy units) should be the same. In this case, however, the emission quantum yield is high ($\Phi = 0.35$ in D_2O solution at 300 K) and the equilibrium observed in $[\text{Tb}\subset\mathbf{1}]^{3+}$, if any, seems to play a less important role. By using eqns. (8) and (9), a value close to unity is obtained for $\eta_{\text{en.tr.}}$, and also for $\eta_{\text{triplet}\rightarrow\text{metal}}$, if in eqn. (10) $\eta_{\text{singlet}\rightarrow\text{triplet}}$ is taken to be ~1 as in $[\text{Tb}\subset\mathbf{1}]^{3+}$. Analogous considerations should be valid for the $[\text{Tb}\subset\mathbf{7}]^{3+}$ complex, in which no lifetime temperature dependence is present. Yet, the $\eta_{\text{en.tr.}}$ value obtained from eqns. (8) and (9) ($\eta_{\text{en.tr.}}$ ~0.38) is lower than for $[\text{Tb}\subset\mathbf{5a}]^{3+}$. However, in this case, the lifetime value in D_2O at 77 K used in eqn. (9) could not correspond to the radiative lifetime because of vibronic contributions still present under these conditions [45]. In such a hypothesis, if the value commonly obtained for the radiative lifetime in Tb^{3+} complexes is used, $\eta_{\text{en.tr.}}$, and therefore $\eta_{\text{triplet}\rightarrow\text{metal}}$, increase by a factor of two. In the case of the complex $[\text{Tb}\subset\mathbf{10}]^{3+}$, in which no equilibrium can be envisaged (Sect. E), the $\eta_{\text{en.tr.}}$ value obtained from eqns. (8) and (9) is 0.37. Since η_{isc} of the free ligand is not known, using eqn. (10) we can only estimate that $\eta_{\text{triplet}\rightarrow\text{metal}} \geqslant 0.37$. This value shows that, in this complex, which contains a completely different chromophore, the ligand–metal interaction in the excited states is nearly as efficient as in complexes containing only bpy units.

Let us now consider the Eu^{3+} complexes. First of all, it is noticeable that, for the $[\text{Eu}\subset\mathbf{1}]^{3+}$ cryptate, the energy transfer efficiency is much lower than for the $[\text{Tb}\subset\mathbf{1}]^{3+}$ cryptate. Such behaviour may be explained taking into account the involvement of LMCT states, which are known to lie at relatively low energies in Eu^{3+} complexes. These states could deactivate the ligand singlet excited states, thus making $\eta_{\text{singlet}\rightarrow\text{triplet}} < 1$ (differing from that assumed in $[\text{Tb}\subset\mathbf{1}]^{3+}$) and/or the ligand triplet excited state, so that $\eta_{\mathrm{triplet}\rightarrow\mathrm{metal}}$ could be lower than the unit value found for the Tb^{3+} complex. Analogous considerations seem to be valid for the other Eu^{3+} complexes. Complexes containing only the bpy chromophoric unit show similar efficiencies except the $[Eu \subset \mathbf{5b}]^{3+}$ complex, for which the much lower value may be ascribed to the presence of the methyl groups. For most complexes of ligands incorporating heterocyclic *N*-oxide groups (with the exception of $[Eu \subset \mathbf{6}]^{3+}$, in which the methyl groups may play the same role as in $[Eu \subset \mathbf{5b}]^{3+}$) the energy transfer efficiency is considerably higher. Note that this quantity is never unity, suggesting that ligand-to-metal charge-transfer states still play a role. However, such a role seems to be less important in view of a more efficient population of the lowest triplet state due to the presence of $bpyO_2$- and $biqO_2$-localized levels or because a closer approach between the ligand and the metal ion could give rise to a higher value of $\eta_{\mathrm{triplet}\rightarrow\mathrm{metal}}$ (see Sect. E). The exceedingly low value for the $[Eu \subset \mathbf{10}]^{3+}$ complex suggests a very efficient deactivation of the ligand excited states via LMCT states. (Note that, for the analogous $[Tb \subset \mathbf{10}]^{3+}$ complex, $\eta_{\mathrm{en.tr.}}$ is about three orders of magnitude higher.)

In order to discuss the metal luminescence, the radiative and non-radiative decay rate constants of the $^5D_0$ Eu^{3+} and $^5D_4$ Tb^{3+} emitting states have been calculated using eqns. (5)–(7) (Table 3). Concerning the radiative rate constants, we can notice that these values are higher for the Eu^{3+} than for Tb^{3+} complexes. This is in line with what is usually observed because of the mixing of the $^5D_0$ emitting state with ligand-to-metal charge-transfer states in Eu^{3+} complexes [7] and the much less efficient mixing of the $^5D_4$ emitting state with f–d excited states in Tb^{3+} complexes [7]. The k_r values differ from one another more in the Eu^{3+} than in the Tb^{3+} complexes (with the exception of $[Tb \subset \mathbf{7}]^{3+}$, see below), in agreement with the larger effect of the ligand on the energy of the LMCT than f–d states. The effect of the LMCT states on the radiative rate constants is evident, considering that the Eu^{3+} complexes containing the $bpyO_2$ or $biqO_2$ unit show higher k_r values than those containing only bpy units, in line with the expected energy values of their LMCT states.

The high k_r values shown by the $[Eu \subset \mathbf{7}]^{3+}$ and $[Tb \subset \mathbf{7}]^{3+}$ complexes are ascribed to the presence of vibronic contributions involving C—H bonds [45], which are not taken into account in the assumption introduced for the determination of the radiative lifetime according to eqn. (5).

As to the rate constant of the temperature-dependent deactivation process, it is worthwhile to recall that, as discussed in Sect. B, in the presence of equilibria between the emitting states and other excited states, its values cannot be obtained from eqn. (6). Nevertheless, we think that, for a homogeneous series of complexes, the values obtained from eqn. (6) may be used to discuss the relative importance of the temperature-dependent decay. Following this approach, in Table 3 the values obtained using eqn. (6) (hereafter indicated as $k^*_{\mathrm{nr}}(\mathrm{T})$) are presented regardless of whether the equilibrium is supposed to be present or not, and the cases in which the equilibrium may be present are indicated.

Among the Eu^{3+} complexes, the $k_{nr}^{*}(T)$ term is negligible for complexes containing only bpy units (with the exception of $[Eu \subset \mathbf{7}]^{3+}$, see below). However, this term becomes important in analogous compounds containing *N*-oxide groups. A possible explanation of such behaviour rests on the deactivation of the $^5D_0$ Eu^{3+} emitting state via low-lying LMCT states (in principle, this process may involve an equilibrium). In fact, in these complexes the bpy→Eu^{3+} LMCT states are expected to lie at lower energies than in complexes containing only bpy units because the reduced donor capability of the *N*-oxide-containing moiety leaves the europium ion more positive. According to this viewpoint, the increase of $k_{nr}^{*}(T)$ in going from $[Eu \subset \mathbf{2}]^{3+}$ to $[Eu \subset \mathbf{3}]^{3+}$ may be accounted for by the introduction of the electron-withdrawing carboxymethyl substituent. For the complex $[Eu \subset \mathbf{7}]^{3+}$, the high value of $k_{nr}^{*}(T)$ is most likely due to deactivation of the metal excited state via LMCT levels involving the aliphatic nitrogens, as observed in the $[Eu \subset 2.2.1]^{3+}$ cryptate [31].

In the case of the Tb^{3+} complexes, the temperature-dependent deactivation process is important only for $[Tb \subset \mathbf{1}]^{3+}$ and $[Tb \subset \mathbf{5a}]^{3+}$. As far as the $[Tb \subset \mathbf{1}]^{3+}$ complex is concerned, among the complexes examined in this article, it is the only one for which the nature of the thermally activated decay process has been proved. As discussed in Sect. E, such a process consists of the deactivation of the emitting level via an equilibrium involving the lowest triplet level of the ligand. From kinetic data, a value of $1.6 \times 10^5\ s^{-1}$ has been obtained for the rate constant of the thermally activated metal-to-ligand back energy transfer [22]. The comparison between this value and the value obtained from eqn. (5) ($1.3 \times 10^3\ s^{-1}$, Table 3) clearly shows the importance of the equilibrium mentioned above in this complex. By analogy, we think that the decay process described for $[Tb \subset \mathbf{1}]^{3+}$ is effective also in the $[Tb \subset \mathbf{5a}]^{3+}$ complex. In this complex, however, $k_{nr}^{*}(T)$ is lower than in $[Tb \subset \mathbf{1}]^{3+}$, in agreement with the higher value of the quantum yield. Note that, in the $[Tb \subset \mathbf{7}]^{3+}$ complex, in which $k_{nr}^{*}(T)$ is negligible, the triplet excited state of the ligand lies at higher energy than in the $[Tb \subset \mathbf{1}]^{3+}$ and $[Tb \subset \mathbf{5a}]^{3+}$ complexes [45].

For both the Eu^{3+} and Tb^{3+} complexes of the calixarene ligand **10**, $k_{nr}^{*}(T)$ is negligible, showing that such a ligand does not introduce excited states which can be thermally populated from the emitting state.

Finally, we will discuss the importance of the vibronic deactivation mechanism involving the O−H groups. To this end, we will directly consider the number of solvent (water or methanol) molecules coordinated to the metal ion (*n* in Table 3) and compare the shielding properties of the various ligands.

For complexes of ligands containing only bpy units the values of the number of coordinated water molecules show that the cryptand ligand **1** shields the metal ion from interaction with water less efficiently than the branched-macrocyclic ligands **5a** (we refer to its complex with Eu^{3+}, see Sect. E) and **7**. Most likely, the latter ligands compete better with water molecules because of their less rigid structures. In contrast, the podand ligands **8** and **9** are so inefficient in such a competition that their complexes are unstable in water. This viewpoint is supported by the observation that the Eu^{3+} and Tb^{3+} complexes of the ligand 7 do not coordinate any water molecule while the $[Eu\subset\mathbf{8}]^{3+}$ complex, whose ligand contains three pendant bpy units as ligand 7, is unstable in water. The triazacyclononane ring would introduce additional flexibility, which allows the bpy units to surround the metal ion more effectively. In methanol, the values of the number of coordinated solvent molecules are similar to one another. This fact may be related to the weaker coordination ability and larger size of methanol compared with water.

The introduction of *N*-oxide groups causes a decrease in the number of coordinated water molecules. Water coordination may be hampered by the steric hindrance and, possibly, the negative charge of the oxygen atoms. As far as ligand **10** is concerned, it shields the metal ion relatively well, but its complexes are rather unstable in water.

G. CONCLUSIONS

The processes involved in the conversion of UV light absorbed by the ligands into visible light emitted by the metal ions of the complexes reviewed here are schematized in Fig. 5, in which pathways responsible for most important nonradiative losses are boxed. On the whole, the results have shown that the nonradiative deactivations due to LMCT states in the Eu^{3+} complexes seem to be more difficult to suppress than those due to the ligand triplet states in the Tb^{3+} complexes. Therefore, Tb^{3+} complexes should be more promising emitting species than Eu^{3+} complexes, also considering that deactivation via vibronic coupling is less efficient for the Tb^{3+} ion.

Among the complexes examined in this study, the most intense luminescence is shown by the $[Eu\subset 4]^{3+}$ and $[Tb\subset 7]^{3+}$ complexes. This conclusion is drawn considering the efficiency of conversion of incident light into emitted light. This quantity, together with the efficiency of absorption and emission, is reported in Table 4 for several significant complexes in dilute solutions. Since the emission efficiency could further increase only by a factor of a few units, more efficient chromophores would be required to obtain a substantial gain in luminescence.

Considering that the main application probably lies in the use of Eu^{3+} and Tb^{3+} complexes as luminescent labels in fluoroimmunoassay, it will also be necessary to take into account the possible effects that both the attachment of the label to the biological species and the serum medium (in which the measurements are to be performed) may have on the luminescence intensity and on the chemical stability of the complexes. These aspects, in addition to the photophysical behaviour of the label, are under investigation [50], as well as further elaboration of more complex luminescent devices.

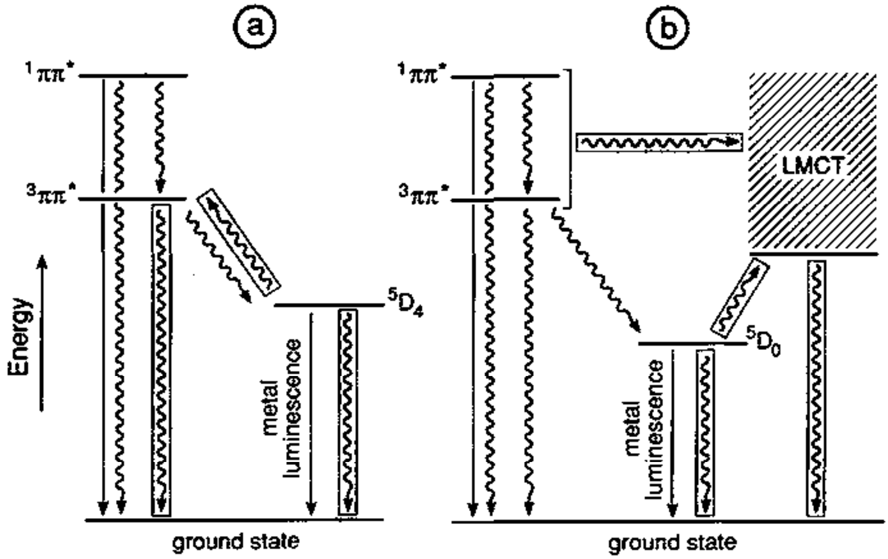

Fig. 5. Scheme of the deactivation processes involved in the conversion of the light absorbed in the ligand into light emitted by the metal ion in (a) Tb^{3+} and (b) Eu^{3+} complexes. The $^1\pi\pi^*$ state is the ligand excited state obtained upon excitation and the $^3\pi\pi^*$ state is the ligand excited state involved in the ligand-to-metal energy transfer. The $^5D_4$ and $^5D_0$ excited states are the luminescent states for the Tb^{3+} and Eu^{3+} ions, respectively. The LMCT excited states are the ligand-to-metal energy transfer states in the Eu^{3+} complexes.

TABLE 4

Incident light–emitted light conversion[a]

Compound	Absorption efficiency[b] (%)	Emission efficiency[c] (%)	Overall efficiency (%)
$[Eu\subset\mathbf{9}]^{3+}$	8.7	0.3	0.03
$[Tb\subset\mathbf{10}]^{3+}$	0.25	20	0.05
$[Eu\subset\mathbf{1}]^{3+}$	6.2	2	0.12
$[Tb\subset\mathbf{1}]^{3+}$	6.5	3	0.20
$[Eu\subset\mathbf{2}]^{3+}$	4.5	15	0.68
$[Eu\subset\mathbf{5a}]^{3+}$	8.0	10	0.80
$[Eu\subset\mathbf{4}]^{3+}$	4.5	20	0.90
$[Tb\subset\mathbf{7}]^{3+}$	4.6	37	1.7

[a] Evaluated for 1.0×10^{-6} M water solutions and 1 cm optical length.
[b] Evaluated in correspondence with the λ_{max} values shown in Table 3.
[c] Obtained from the experimental quantum yields shown in Table 2.

ACKNOWLEDGEMENTS

The authors wish to thank Prof. V. Balzani, Prof. L. Moggi, and Dr. L. De Cola for their critical reading of the manuscript. This work was supported by the Ministero della Università e della Ricerca Scientifica e Tecnologica (Italy) and by CIS Biointernational (France).

REFERENCES

1 J.-M. Lehn, Angew. Chem. Int. Ed. Engl., 29 (1990) 1304.
2 N. Sabbatini and M. Guardigli, Mater. Chem. Phys., 31 (1992) 13.
3 L.C. Thompson, in K.A. Gschneider and L. Eyring (Eds.), Handbook on the Physics and Chemistry of Rare Earths, Vol. 3, North-Holland, Amsterdam, 1979, p. 209.
4 W.T. Carnall, in K.A. Gschneider and L. Eyring (Eds.), Handbook on the Physics and Chemistry of Rare Earths, Vol. 3, North-Holland, Amsterdam, 1979, p. 171.
5 R. Reisfeld, Struct. Bonding (Berlin), 22 (1975) 123.
6 R. Reisfeld and C.K. Jørgensen, Inorg. Chem. Concepts, 1 (1977) 1.
7 G. Blasse, in K.A. Gschneider and L. Eyring (Eds.), Handbook on the Physics and Chemistry of Rare Earths, Vol. 4, North-Holland, Amsterdam, 1979, p. 237.
8 B.R. Judd, Phys. Rev., 127 (1962) 750.
G.S. Ofelt, J. Chem. Phys., 37 (1962) 511.
9 W. Strek, J. Chem. Phys., 76 (1982) 5856.
10 F.K. Freed, Top. Appl. Phys., 15 (1976) 23.
11 G. Stein and E. Wurzberg, J. Chem. Phys., 62 (1975) 208.
12 Y. Haas and G. Stein, J. Phys. Chem., 75 (1971) 3677.
13 W.DeW. Horrocks and D.R. Sudnick, J. Am. Chem. Soc., 101 (1979) 334.
14 W.DeW. Horrocks and D.R. Sudnick, Acc. Chem. Res., 14 (1981) 384.
15 R.C. Holz, C.A. Chang and W.DeW. Horrocks, Inorg. Chem., 30 (1991) 3270.
16 G. Blasse, Struct. Bonding (Berlin), 26 (1976) 43.
17 B. Dietrich, J.-M. Lehn and J.P. Sauvage, Tetrahedron, 29 (1973) 1647.
18 J.-M. Lehn and J.P. Sauvage, J. Am. Chem. Soc., 97 (1972) 6700.
19 B. Alpha, J.-M. Lehn and G. Mathis, Angew. Chem. Int. Ed. Engl., 26 (1987) 266.
20 N. Sabbatini, S. Perathoner, V. Balzani, B. Alpha and J.-M. Lehn, in V. Balzani (Ed.), Supramolecular Photochemistry, Reidel, Dordrecht, 1987, p. 187.
21 J.-M. Lehn, in V. Balzani (Ed.), Supramolecular Photochemistry, Reidel, Dordrecht, 1987, p. 29.
22 B. Alpha, R. Ballardini, V. Balzani, J.-M. Lehn, S. Perathoner and N. Sabbatini, Photochem. Photobiol., 52 (1990) 299.
23 V. Balzani and F. Scandola, Supramolecular Photochemistry, Ellis Horwood, Chichester, 1991, p. 326.
24 E. Soini and I. Hemmilä, Clin. Chem., 25 (1979) 353.
25 J.-C.G. Bünzli, in J.-C.G. Bünzli and G.R. Choppin (Eds.), Lanthanide Probes in Life, Chemical and Earth Sciences, Elsevier, Amsterdam, 1989, Chap. 7.
26 J.L. Toner, in J. Atwood (Ed.), Inclusion Phenomena and Molecular Recognition, Plenum Press, New York, 1990, p. 185.
27 N. Sabbatini, S. Dellonte, M. Ciano, A. Bonazzi and V. Balzani, Chem. Phys. Lett., 107 (1984) 212.
28 G. Blasse, M. Buys and N. Sabbatini, Chem. Phys. Lett., 124 (1986) 538.

29 N. Sabbatini, S. Dellonte and G. Blasse, Chem. Phys. Lett., 129 (1986) 541.

30 P.J. Breen and W.DeW. Horrocks, Inorg. Chem., 22 (1983) 536.

31 N. Sabbatini, S. Perathoner, G. Lattanzi, S. Dellonte and V. Balzani, J. Phys. Chem., 91 (1987) 6136.

32 J.-C. Rodriguez-Ubis, B. Alpha, D. Plancharel and J.-M. Lehn, Helv. Chim. Acta, 67 (1984) 2264.

33 B. Alpha, PhD Thesis, University of Strasbourg, 1987.

34 I. Bkouche-Waksman, J. Guilhem, C. Pascard, B. Alpha, R. Deschenaux and J.-M. Lehn, Helv. Chim. Acta, 74 (1991) 1163.

35 B. Alpha, V. Balzani, J.-M. Lehn, S. Perathoner and N. Sabbatini, Angew. Chem. Int. Ed. Engl., 26 (1987) 1266.

36 G. Blasse, G.J. Dirksen, N. Sabbatini, S. Perathoner, J.-M. Lehn and B. Alpha, J. Phys. Chem., 92 (1988) 2419.

37 G. Blasse, G.J. Dirksen, D. van der Voort, N. Sabbatini, S. Perathoner, J.-M. Lehn and B. Alpha, Chem. Phys. Lett., 146 (1988) 347.

38 J.-M. Lehn and C.O. Roth, Helv. Chim. Acta, 74 (1991) 572.

39 L. Prodi, M. Maestri, V. Balzani, J.-M. Lehn and C. Roth, Chem. Phys. Lett., 180 (1991) 45.

40 J.-M. Lehn, C.D. Roth, M. Guardigli and N. Sabbatini, unpublished results, 1992.

41 J. Guilhem, C. Pascard, J.-M. Lehn and C.O. Roth, unpublished results, 1992.

42 R. Ziessel and J.-M. Lehn, Helv. Chim. Acta, 73 (1990) 1149.

43 J.-M. Lehn and C.O. Roth, unpublished results, 1991.

44 V. Balzani, J.-M. Lehn, J. van de Loosdrecht, A. Mecati, N. Sabbatini and R. Ziessel, Angew. Chem. Int. Ed. Engl., 30 (1991) 190.

45 L. Prodi, M. Maestri, R. Ziessel and V. Balzani, Inorg. Chem., 30 (1991) 3798.

46 M. Pietraszkiewicz, S. Pappalardo, P. Finocchiaro, A. Mamo and J. Karpiuk, J. Chem. Soc. Chem. Commun., (1989) 1907.
J.-M. Lehn and C.O. Roth, unpublished results, 1989.

47 V. Balzani, E. Berghmans, J.-M. Lehn, N. Sabbatini, R. Terörde and R. Ziessel, Helv. Chim. Acta, 73 (1990) 2083.

48 G. Calestani, F. Ugozzoli, A. Arduini, E. Ghidini and R. Ungaro, J. Chem. Soc. Chem. Commun., (1985) 344.
A. Arduini, E. Ghidini, A. Pochini, R. Ungaro, G.D. Andreetti, G. Calestani and F. Ugozzoli, J. Inclusion Phenom., 6 (1988) 119.

49 N. Sabbatini, M. Guardigli, A. Mecati, V. Balzani, R. Ungaro, E. Ghidini, A. Casnati and A. Pochini, J. Chem. Soc. Chem. Commun., (1990) 878.

50 G. Mathis, C. Dumont and E. Jolv, Patent PCT W092-01224.